Volume 16, Issue 1, 162503 (1-14)

International Journal of Nano Dimension (IJND)

https://dx.doi.org/10.57647/j.ijnd.2025.1601.03

Microwave assisted biosynthesis of nickel nanoparticles from beetle *Luprops tristis* defensive gland secretion: Structural characterization, multifunctional bioactivities, and glucose sensing applications

Ovungal Sabira[1], Anthyalam Parambil Ajaykumar[1]*, Kanakkassery Balan Roy[2], Pandikkadan Ayyappan Janish[1], Kaladharan Perumpaparampil Viswanathan[3]

[1]*Division of Biomaterial Sciences, Department of Zoology, Sree Neelakanta Government Sanskrit College, Pattambi, Palakkad, Kerala, India.*
[2]*Department of Chemistry, Sree Neelakanta Government Sanskrit College, Pattambi, Palakkad, Kerala, India.*
[3]*Department of Statistics, Maharajas College, Ernakulum, Kerala, India.*

*__Corresponding author:__ ajaykumar@sngscollege.org

Original Research

Received:
2 August 2024
Revised:
8 September 2024
Accepted:
13 September 2024
Published online:
10 January 2025

Abstract:

Researchers are currently interested in the biosynthesis of nanoparticles (NPs) due to their importance to develop cost-efficient, eco-friendly, and effective synthesis methods. The primary aim of this current investigation is to produce nickel nanoparticles (NiNPs) by synthesising them from the defensive secretion acquired from the beetle *Luprops tristis* (*L. tristis*). The resulting nickel nanoparticles, referred to as LNiNPs, are recognized as being biosynthesized. The synthesis of LNiNPs from pure metal was verified by UV-Vis spectroscopy, and FTIR analysis indicates the functional groups attached to the nanoparticles that serve as the reducing and capping agents. Analysis using cyclic voltammetry ensures the reducing property of the phenolic compounds present in the defensive gland extract of the beetle. Scanning electron microscopy (SEM) and transmission electron microscopy (TEM) revealed the spherical shape of biosynthesized LNiNPs with an average size of 18 nm, while dynamic light scattering (DLS) analysis indicated a hydrodynamic size of approximately 48 nm. Zeta potential analyses of the nanoparticles show that biosynthesized nanoparticles are more stable. Non enzymatic glucose sensing study by differential pulse voltammetry shows a lower detection limit of 1.31 µM. The disc diffusion antibacterial assay of LNiNPs demonstrated a dose-dependent inhibition of bacterial growth, with antimicrobial activity increasing proportionally to the concentration of LNiNPs. Chromosomal aberration experiments using LNiNPs revealed chromosomal aberrations in *Allium sepa* L. DPPH assay supported strong antioxidant properties of LNiNPs at higher doses. Additionally, it shows dose-dependent cytotoxicity against Dalton's lymphoma ascites cells (DLA cells). Despite the fact that *L. tristis* annoys people, its secretion can be used to bio synthesise nickel nanoparticles, which offer additional benefits such as antibacterial, antioxidant, and anticancer, glucose sensing properties.

Keywords: Beetle; Defensive gland secretion; Glucose sensing; *Luprops tristis*; Nickel nanoparticles

1. Introduction

Nanotechnology has emerged as a groundbreaking field, providing a wide range of applications across various scientific and technological domains. Nanomaterials, in particular, offer numerous advantages over bulk materials, making their use in nanodevices especially promising [1]. The outstanding properties of nanoparticles are due to the fact that quantum effects turn out to be dominant and surface to volume size ratio is changed when bulk material is converted into nano-size [2]. The principles underlying the nanotechnology are top-down and bottom-up approaches [3]. To reduce environmental hazards and offer several advan-

tages over conventional methods, an eco-friendly approach is necessary, with microwave-assisted techniques being a prominent example. To reduce environmental hazards and offer several advantages over conventional methods, an eco-friendly approach is necessary, with microwave-assisted techniques being a prominent example [4–9]. In this regard, the utilization of biological methods based on plants and microorganisms has received considerable interest due to their environmental safety, low cost, and ease of application on a large scale. There have been numerous reports of reducing and capping agents that are natural, green, and safe for the environment being employed in the synthesis of nanomaterials [10, 11].

Numerous microorganisms and plant extracts have been investigated primarily for the manufacturing of metal nanoparticles, quantum dots and other materials following the boom in biosynthesis of nanoparticles and also Secretions from various organisms, such as toxins and venoms from snakes, marine species, and bees, have been employed in the synthesis of nanoparticles [11–17]. Metal nanoparticles, including those of nickel, copper, and iron, tend to be relatively hard due to their susceptibility to oxidation. Nickel, a significant transition metal, has nanoparticles that find extensive applications in various fields such as permanent magnets, magnetic fluids, magnetic recording media, solar energy absorption, fuel cell electrodes, catalysts, and biological activity [18]. Nickel nanoparticles, known for their chemical stability, strong binding affinity, and ferromagnetic properties, are crucial for research in biomedical applications like cell isolation, drug delivery, and magnetic resonance imaging [19]. Due to all these reasons NiNPs has attracted great focus of many scientists for its synthesis. Various methods were developed for the synthesis of NiNPs [20, 21], including sol-gel, micro-emulsion, hydrothermal, sonochemical, vapour phase and co-precipitation methods [22–26]. Researchers worldwide are developing nanoparticles (NiNPs) for synthesizing transition metals due to their catalytic properties, biological activities, and reusable catalyst. The stability of nanoparticles depends on synthesis method, storage environment, and stabilizing agents [27, 28].

Beetles encompass a diverse array of chemical compounds utilised for medicinal purposes, including antibacterial, antitumor, antifungal, anti-obesity, anti-adipogenic, and anti-inflammatory applications. The key components consist of a wide spectrum of substances such as antimicrobial peptides (AMPs), cantharidin, blapsols, pederin and harmoniasin [29–33], among others responsible for the biomedical effects. To express it more formally: antimicrobial peptides (AMPs) possessing antimicrobial, antiviral, antifungal, and diverse properties have been identified, as documented by Adamski et al. Beetle defensins and AMPs have shown effectiveness against various microorganisms, including Pseudomonas aeruginosa, MRSA, and bacteria. Studies by Adamski et al. and Nenadić investigated the antibacterial properties of Calosoma sycophanta's pygidial gland secretion. Blapsols, found in beetles, are used for treating various conditions [34, 35]. The biomedical potential of beetle secretions holds considerable promise and may find practical applications in the near future [36–39].

Recent studies in our laboratory indicated that the defensive gland secretion of *L. tristis* has the ability to synthesize silver nanoparticles. And has the ability for the synthesis of graphene layers. These secretions frequently have distinctive characteristics including antibacterial, anticancer, and antioxidant activity [39–42], which makes them desirable candidates for a variety of scientific studies. The aim of the current study is to synthesize nickel nanoparticles (NiNPs) from the defensive gland extract of the beetle *L. tristis*, referred to as LNiNPs. Using the defensive gland extract in the production of NiNPs offers several benefits. Firstly, it provides an environmentally friendly alternative to conventional chemical methods, reducing the need for hazardous chemicals and minimizing toxic waste. Additionally, this approach allows for the incorporation of organic bioactive substances, potentially imparting unique properties and applications to the synthesized nanoparticles. Furthermore, utilizing beetle defensive gland extract without harming the insect aligns with the principles of sustainable and green chemistry, promoting the synthesis of eco-friendly nanomaterials. Although nickel nanoparticles derived from insect secretions have not been previously recorded, this innovation holds promise for advancements in biomedical science.

2. Materials and methods

2.1 Preparation of defensive gland extract of *L. tristis*

The experimental insect, *Luprops tristis*, was gathered from college campus, Pattambi (10.809526, 76.199281), Kerala, India. The beetle, *L. trisis* (Family: Tenebrionidae, Order: Coleoptera) is a darkling beetle that feeds on plant debris and is distributed throughout India as shown in Fig. 1(a-d). The adult beetle is around 8 mm long and is black. Typically, they pose no threat to people. They release a defensive phenolic fluid that burns the skin when squeezed or pulled up. Phenolic compounds in the extract have high potential for acting as significant reducing and capping

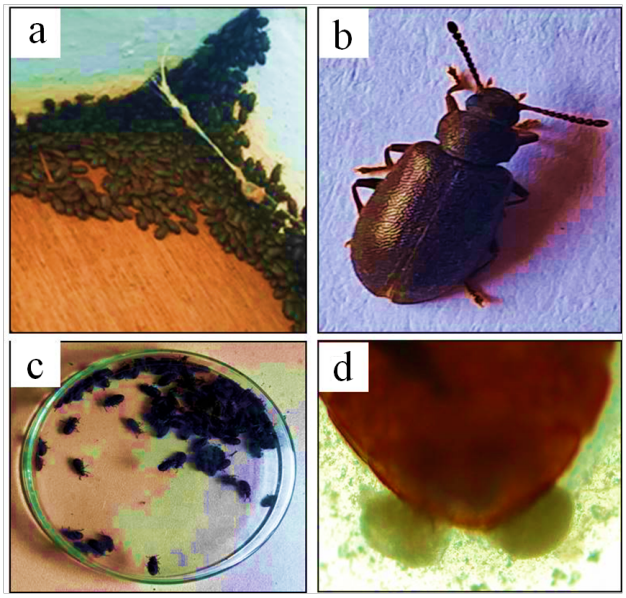

Figure 1. Experimental organism, (a, c) A colony of *L. tristis*, (b) *Luprops tristis* (d) Extruded defensive gland.

agents. They are infamous for their ability to complicate living conditions when big groups enter farm houses, roofs of hoses, etc. The insects were hand-picked and stored in perforated insect boxes following collection and then transported to the laboratory for the extraction of defensive gland. The defensive secretion was collected from the beetle without causing any harm to them. Defensive glands of the insects extruded out by gentle pressing on the abdomen; the glandular secretion collected to eppendorff (300 µL capacity) tube containing deionized water by pressing on the extruded glands without any contamination from fecal matter. These extract used for the synthesis of NiNPs.

2.2 Fabrication of LNiNPs

The *Luprops tristis*-mediated nickel nanoparticles (LNiNPs) were prepared by first extracting the gland secretions from 30 beetles having approximate concentration of 30 µg into 300 µL of distilled water. Separately, a 0.01 molar (M) nickel chloride solution was prepared in deionised water. For the reaction mixture, 300 µL of the defensive gland extract (equivalent to 30 glands) was combined with 600 µL of the 0.01 M nickel chloride solution. This mixture was then heated in a microwave (LG-MS-2029 UW) at 350 W for 15 minutes. During this process, the solution's color changed from purple to reddish-brown, visually indicating the formation of LNiNPs. The resulting nanoparticles were subsequently subjected to ultracentrifugation to remove any unreacted materials and impurities and 72-hour dialysis using a dialysing membrane. The purified sample was used for various analyses and characterizations at different concentrations.

2.3 Characterization of LNiNPs

2.3.1 Structural characterisation

The reduction of nickel chloride to nickel nanoparticles by defensive gland secretion of *L. tristis* were characterized by UV-Vis spectroscopy (PerkinElmer UV WinLab), compounds bind with the biosynthesized nickel nanoparticles for the stabilization were identified by FTIR spectroscopy (PerkinElmer IR). The morphology and size details of the nanoparticles were identified by SEM and TEM (JEOL JEM-2100). Stability is an important factor in case of nanoparticles which was measured by zeta potential analysis.

2.3.2 Electrochemical studies – Differential pulse votammetry (DPV)

An Electrochemical workstation (Instrument Model DY2113 developed by Digi-Ivy) was used to conduct DPV measurements. Using a three-electrode cell setup with a platinum foil counter electrode, an Ag/AgCl reference electrode, and a working electrode coated with LNiNPs in 10 mL of phosphate buffer saline. The potential was applied from $+1.000$ to -1.000 at the initial and final stages. Measurements of glucose concentration ranging from 10 mM to 70 mM were plotted, and calibration linear relationships between DPV current output and glucose concentration were plotted. Using the equation LOD = (3*SD)/Slope of the curve, it was possible to determine the limit of the detection of LNiNPs sensor.

2.3.3 Biological applications

2.3.3.1 Antibacterial analysis

The dose-dependent antibacterial activity of LNiNPs was assessed using a disc diffusion assay against Gram-negative *Klebsiella pneumoniae* (ATCC 700603) and Gram-positive *Staphylococcus aureus* (ATCC 33591). Agar plates were prepared by dissolving 4 g of agar powder in 100 mL of distilled water and pouring the solution into four autoclaved Petri dishes. Pure microbial cultures were sub-cultured on nutrient agar and evenly swabbed on individual plates. Four concentrations of LNiNPs (5 µg, 10 µg, 15 µg, and 20 µg) were applied to 5 mm filter paper discs, which were then dried and placed on the culture plates. Tetracycline served as a positive control and the solvent without nanoparticle served as negative control. The plates were incubated for 16 hours at 35 °C, and the inhibitory zones were measured. The assay was performed in triplicate, and the standard deviation of the results was calculated.

2.3.3.2 Antioxidant analysis

The assessment of free radical scavenging capacity was carried out using the DPPH assay. DPPH solution (2 mL) was blended with varying concentrations of LNiNPs (20 µg, 40 µg, 60 µg, 80 µg, 100 µg), while a reference solution containing ascorbic acid dissolved in distilled water, used as the positive control, was prepared. Subsequently, the solutions were subjected to UV spectroscopic analysis (PerkinElmer UV-WinLab) following a 30-minute incubation period in darkness. The transition of DPPH color from deep violet to pale yellow indicated the scavenging activity of LNiNPs, which was further confirmed through UV spectroscopic analysis at 517 nm. The scavenging activity was quantified using the equation;

$$S\% = \frac{(A_{control} - A_{sample})}{A_{control}} \times 100$$

The concentration of sample required to produce 50% scavenging activity (IC_{50} value) obtained from the graph through the linear regression equation. The assay was run three times, and the results' standard deviation was calculated.

2.3.3.3 Chromosomal aberration assay

Chromosomal aberration studies utilizing the root nodules of *Allium cepa* (onion), a well-established bioindicator for cytogenetic studies, meticulously assessed the potential genotoxic effects of the synthesized LNiNPs when introduced into the environment. Fresh *A. cepa* bulbs were used to study the effects of biosynthesized LNiNPs on mitosis. Equal-sized bulbs, selected from a population of common onion bulbs ($2n = 16$), were incubated in LNiNPs solutions at concentrations of 100 µg, 200 µg, 300 µg, 400 µg, and 500 µg, while control bulbs were incubated in distilled water. Once the roots reached $2-3$ cm in length, chromosomal impact studies were performed. The roots were cut from the root primordial disc, and a thin film of onion cells was prepared using the squash technique. The root nodules were stained with acetocarmine and methylene blue, and 1500 cells from the three best preparations were analyzed three times. Hydrogen peroxide (H_2O_2) was used as the positive control, and the solvent without nanoparticles was used as

the negative control. Chromosomal alterations were observed under a compound microscope (LEICA ICC50E) and compared to the control group [43–45].

2.3.3.4 Cytotoxicity assay

The cytotoxicity of different concentrations of nanoparticles (2.5 µg - 25 µg) was evaluated using Dalton's lymphoma ascites (DLA) cells. After being removed from the peritoneal cavity of mice with tumors, DLA cells were suspended in 0.1 mL of a viable cell solution and cleaned three times with normal saline. After that, this cell solution was transferred to tubes holding different nanoparticle concentrations, and the final volume was adjusted with phosphate-buffered saline (PBS) to 1 mL. For three hours, the assay mixtures were incubated at 37 °C. Following incubation, each tube received 0.1 mL of 1% trypan blue. Three minutes later, a hemocytometer was used to count the number of live and dead cells. The negative control was a buffer devoid of nanoparticles, whereas the positive control was cyclophosphamide. Assay repeated three times, after which the standard deviation was computed. The Trypan blue assay in DLA cells is commonly used to determine the cytotoxicity of different metal nanoparticles [46, 47].

2.3.3.5 Statistical Analysis and Data Representation

All bioassays were conducted in triplicate to ensure reliability and reproducibility. Data from antimicrobial, anticancer, and chromosomal aberration studies were statistically analyzed and reported as mean ± standard deviation (SD). The mean and standard deviation were calculated for each treatment group, and statistical significance was assessed. Results are presented as mean ± SD in both tabular and graphical formats, with error bars indicating the standard deviation.

3. Results and discussion

The production of nanoparticles has made use of secretions from a variety of organisms, including bees, marine animals, and snakes with venom and toxins. Chitosan nanoparticles loaded with bee venom, for example, have demonstrated promise in the treatment of multidrug-resistant bacteria and anti-MERS-CoV. In a similar vein, chitosan nanoparticles containing the venom of the *Naja naja oxiana* snake have been created, increasing their potential for use in biomedicine. Additionally, increased anticancer activity across a variety of human cancer cell lines has been shown by the creation and investigation of bee venom-loaded nanoliposomes. Another example is the manufacture of anticancerous and anti-inflammatory nanoparticles utilizing jellyfish, as well as the use of nematocyst venom to create anticancer metal nanoparticles [13–17]. In the present study, LNiNPs were made by reducing a nickel chloride solution under the action of an extract from the defensive gland of the insect *Luprops tristis*. The detailed mechanism of the chemical reaction for nickel nanoparticle formation is shown in figure 2 and after the chemical characterization (UV-Vis spectroscopy, Fourier-transform infrared spectroscopy (FTIR), Scanning electron microscopy (SEM), Transmission electron microscopy (TEM) , Zeta potential & DLS analysis, measuring its biochemical applications such as glucose sensing, antibacterial analysis, antioxidant activity, antimitotic activity and anticancer activity.

3.1 Mechanism of nickel nanoparticle formation

Although the defensive gland extract contains aliphatic compounds, most of the compounds are pheromones; we did not consider them for predicting nanoparticle synthesis. Polyphenolic compounds are well-known for their reducing and stabilizing properties, making them more likely to be involved in nanoparticle synthesis. Aliphatic compounds are less reactive in these reduction reactions and are unlikely to significantly contribute to the formation of nickel nanoparticles. Therefore, our study centers on the role of polyphenolic compounds in this process. Several compounds, including 2,5-dimethylhydroquinone, 1,3-dihydroxy-2-methylbenzene, and 2,3-dimethyl-1, 4-benzoquinone, are present in the defensive gland secretion of *L. tristis* [42]. From these phenolic molecules most probably hydroquinone undergoes oxidation by nickel (Fig. 2). A mechanistic overview of the oxidation of dimethyl hydroquinone to the corresponding p-quinone may be advanced as depicted in Fig. 2. As the conversion is observed in the presence of a Ni(II) salt, it may be assumed that the latter is involved in the oxidation directly. The oxidation may be initiated via ligand exchange on Ni by the phenol units. This may be followed by loss of H^+ and the transfer of electrons to nickel. Dimethyl-p-quinone is generated in the process with concomitant reduction of nickel. It may be noted that this is a speculative mechanism at this stage as Ni(II) is not generally considered as a common oxidizing agent.

3.2 Cyclic voltammetry (CV) analysis

The various phenolic compounds present in the defensive gland secretion were oxidized at potential range from 1 to −1 V as shown in cycle voltammogram (Fig. 3) for 0.05 mM standards. The upper scan represents the oxidation of the polyphenolic groups generating a positive current (anode) which interpret the reducing capacity of the compounds, which substantiate the reducing power of defensive gland secretion in the production of nickel nanoparticles.

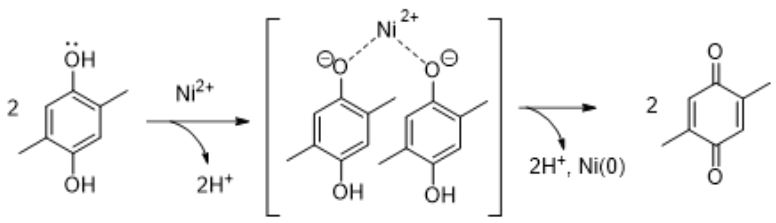

Figure 2. Mechanistic overview of the Ni(II)-mediated oxidation of hydroquinone.

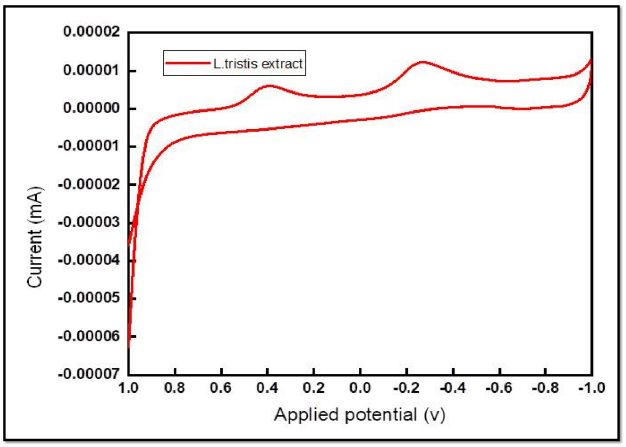

Figure 3. Cyclic voltammetry of defensive gland extract of *L. tristis*.

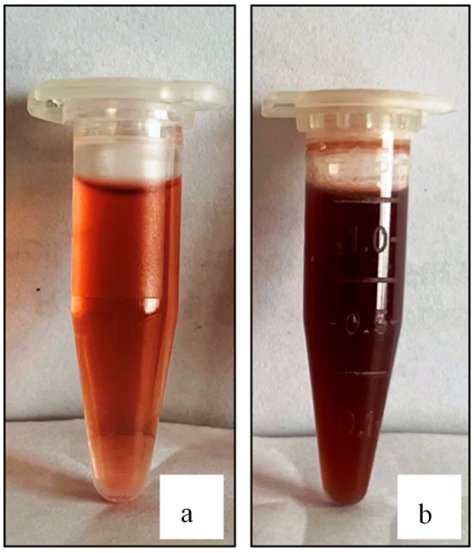

Figure 4. Visible colour change during nickel nano formation (a) Defensive gland secretion with nickel chloride solution (b) Colour change at 15 minutes of MW irradiation.

3.3 Chemical characterization

3.3.1 UV-Vis spectroscopy

The visible colour change of the reaction mixture from purple to reddish brown as shown in Fig. 4(a,b), following microwave irradiation within 15 minutes, was the first indicator of the formation of LNiNPs. This was followed by UV-Vis spectroscopy, the result is shown in Fig. 5. LNiNPs showed maximum absorption peak at the wavelength (λ_{max}) 204 nm, it was due to surface plasmon resonance phenomenon which provides a convenient indication of the formation of LNiNPs. The considerable broadening of the UV-Visible peak revealed that the particles are extremely polydispersed, and this clearly demonstrated the interaction between the metal nickel and the biomolecules present in the gland extract. Helen and Rani synthesized NiNPs in a similar manner using an aqueous nickel sulphate solution and an elephant yam root tuber extract as a capping and reducing agent. The colour of the solution shifted from blue to yellow as NiNP developed, with a UV absorption at 207 nm [48]. The λ_{max} is consistent with other previous researches [49], similar peaks within the range of $200-300$ were obtained for NiNP synthesized from the plants *camellia sinensis* [2] and *Piper longum* [50].

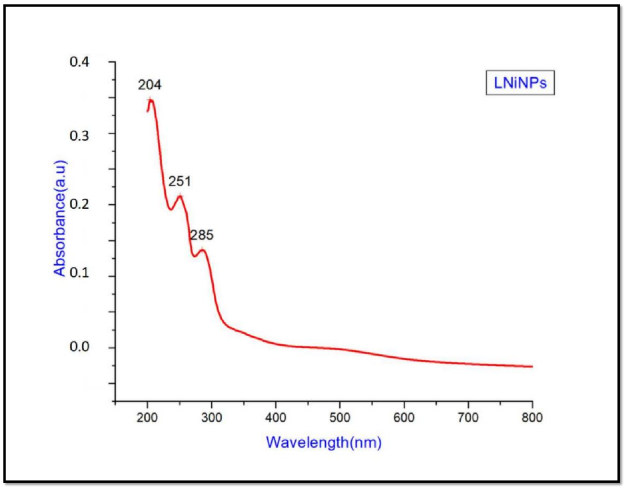

Figure 5. UV-Vis spectrum of LNiNPs.

3.3.2 FTIR analysis of LNiNPs

The functional groups involved in the LNiNP were identified using FT-IR spectroscopy. The gland secretion, secretion with nickel chloride solution and biosynthesised LNiNP solution was subjected to Fourier-transform infrared spectroscopy (FTIR). The resulting spectra revealed the corresponding functional groups, and it was observed that there was minimal difference in the functional groups before and after exposure to microwave irradiation (Fig. 6). The IR spectrum of the defensive gland extract of *L. tristis* exhibited distinct absorption bands at 3425, 2941, 1644, 1407, 1077, and 544 $1/cm$ (Table. 1), revealing the presence of various functional groups. The broad absorption at 3425 $1/cm$ indicates O-H stretching vibrations, pointing to hydroxyl groups typically found in polyphenolic compounds. The band at 2941 $1/cm$ corresponds to C-H stretching vibrations of aliphatic hydrocarbons, while the 1644 $1/cm$ band is characteristic of C=O stretching vi-

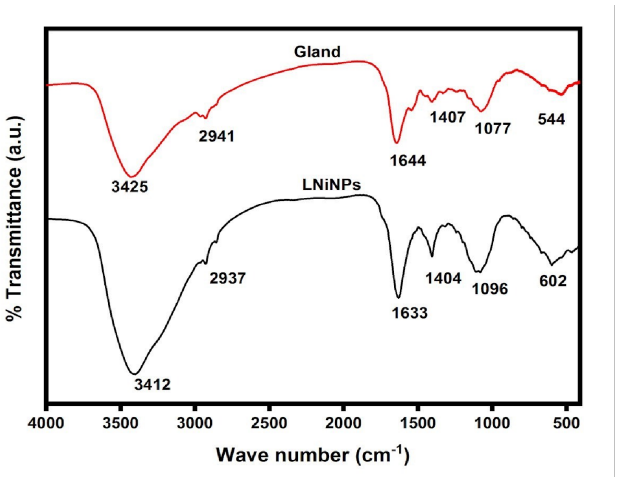

Figure 6. FTIR spectra of LNiNPs compared with FTIR of gland secretion and FTIR of gland secretion + Nickel chloride solution before MW irradiation.

Table 1. Functional groups obtained at different frequency in FTIR.

Frequency	Functional group with vibrations
3412	O-H stretching
2937	CH/CH_2 stretching
1633	O-H bending
1404	C=C bending
1096	C-O stretching
602	Finger print region

brations, indicative of carbonyl groups such as aldehydes, ketones, and carboxylic acids. The peaks at 1407 1/cm and 1077 1/cm are associated with C-H bending vibrations and C-O stretching vibrations, respectively, and the band at 544 1/cm suggests complex molecular vibrations. In the case of the synthesized nickel nanoparticles (LNiNPs), the IR spectrum displayed bands at 3412, 2937, 1633, 1404, 1096, and 602 1/cm. The shifts in these peaks compared to those of the beetle gland extract indicate notable interactions between the biomolecules and nickel ions. Specifically, the O-H stretching vibration peak shifted to 3412 1/cm, the C-H stretching peak to 2937 1/cm, the C=O stretching peak to 1633 1/cm, the C-H bending peak to 1404 1/cm, and the C-O stretching peak to 1096 1/cm. Additionally, the new peak at 602 1/cm, attributed to Ni-O stretching vibrations, confirmed the formation of nickel oxide on the nanoparticle surface. The comparative IR spectroscopy analysis reveals that the defensive gland extract of *L. tristis* contains functional groups such as hydroxyl, carbonyl, and aliphatic hydrocarbons, which play crucial roles in the synthesis and stabilization of nickel nanoparticles (Fig. 6). The shifts in absorption bands in the LNiNPs spectrum suggest that hydroxyl and carbonyl groups are involved in reducing nickel ions to form nanoparticles, while aliphatic hydrocarbons and C-O groups contribute to their capping and stabilization. The new Ni-O stretching vibration peak indicates partial oxidation, resulting in a nickel oxide layer on the nanoparticles, which could enhance their catalytic and electronic properties. These findings highlight the importance of polyphenolic compounds in the extract as effective reducing agents and the role of other functional groups in stabilizing the nanoparticles, providing valuable insights for optimizing synthesis processes and tailoring nanoparticle properties for specific applications [49, 51–54].

3.3.3 Scanning electron microscopy (SEM) & Transmission electron microscopy (TEM)

The morphology of the nanoparticles was visualized using scanning electron microscopy, as depicted in Fig. 7a. The SEM image illustrated the substantial density of NiNPs synthesized through the defensive gland extract of *L. tristis*. These LNiNPs exhibited a relatively spherical shape with a rough surface and displayed a uniform distribution, as evident in Fig. 7. Furthermore, individual nanoparticles tended to aggregate, resulting in the formation of larger nanoparticles. TEM examination (Fig. 7b) was performed to explore the morphology of LNiNPs, revealing an average nanoparticle size of around 18 nm. Previous research, such as that by Duan et al., has also characterized the surface morphology

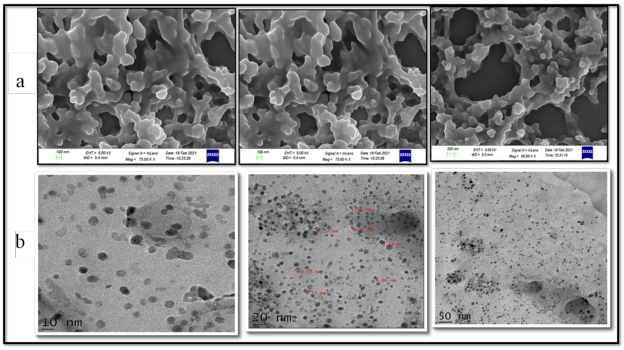

Figure 7. Electron microscopy images (a) Scanning electron microscopy images of LNiNPs. (b) Transmission electron microscopy image of LNiNPs.

of nickel nanoparticles as spherical in shape [55]. Similarly, biosynthesized NiNPs obtained from sources like *Camellia sinensis* [2] and imine capped NiNPs have been reported to exhibit a spherical form as well [56]. Our findings revealed the presence of spherical-shaped nanoparticles; however, previous research indicates a variety of nickel nanoparticle shapes, including irregular polygonal, cylindrical, and spherical forms, often accompanied by particle agglomeration. The presence of diverse shapes in nickel nanoparticles suggests variations in synthesis methods, reaction conditions, and precursor materials, all of which can influence the final nanoparticle morphology [57]. It is also noteworthy that previous research has documented size-controlled nickel nanoparticles spanning a size range from 3 nm to 11 nm [58].

3.3.4 Zeta potential and DLS analysis

Using the nanoparticles analyzer (HORIBA SCIENTIFIC SZ 100), we further investigated the Zeta Potential of LNiNPs to assess their stability [54, 55]. The outcomes reveal a robust stability of −16.5 meV for LNiNPs, as depicted in Fig. 8a. The negative sign of the zeta potential is indicative of this stability, facilitating uptake through electrostatic interactions between the cationic nanoparticles and the cationic membrane. The hydrodynamic size of the stabilized LNiNPs was approximately 48 nm, as determined by DLS analysis, showing a monodisperse distribution, as shown in Fig. 8b. The LNiNPs displayed commendable stability, consistent with findings from prior research regarding the zeta potential [59–63]. Notably, nanoparticles with higher surface charge adhere more securely to cell membranes, leading to increased cellular absorption. Subsequent to adhering to the cell membrane, nanoparticles can be absorbed through various mechanisms like phagocytosis, nonspecific or receptor-mediated endocytosis, or pinocytosis [61]. Multiple well-documented research studies have demonstrated that green-synthesized NiNPs exhibit a negative zeta potential [35, 60, 64–67]. The hydrodynamic diameter of the stabilized LNiNPs, approximately 48 nm as determined by DLS analysis, is notably larger than the size obtained from TEM analysis (Fig. 8b). This discrepancy arises because DLS captures the hydrodynamic radius, including the solvent layer around the nanoparticles, while TEM provides a more precise measurement of the actual

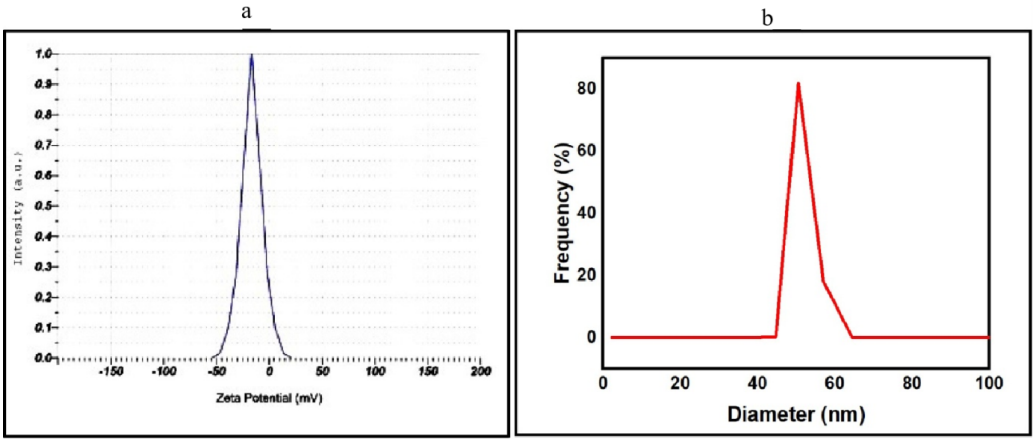

Figure 8. Hydrodynamic size and stability of LNiNPs (a) Zeta potential of LNiNPs (b) DLS graph showing hydrodynamic size of the stabilized LNiNPs.

physical dimensions without the surrounding medium.

3.3.5 Electrochemical glucose sensing by differential pulse voltammetry (DPV)

Diabetes is linked to a number of illnesses, such as tuberculosis, cystic fibrosis, celiac disease, and cardiac issues. These conditions can cause blindness, as well as kidney disorders, which can end in renal failure, nerve damage, foot ulcers, and malignancy [68]. It is crucial to develop a highly sensitive and straightforward method to detect and monitor glucose levels for clinical diagnosis, medicine, and the food sector due to the daily growing health concerns [69]. In this investigation, plots of measurements of the glucose having (3M) concentration from this volume between 10 mM and 70 mM were made (Fig. 9a), and calibration linear relationships between DPV current output and glucose concentration were plotted (Fig. 9b) and limit of detection found to be 1.31 mM. LNiNPs produced in this current study can be used in electrochemical glucose monitors. The binding of glucose molecules to the functionalized LNiNPs can cause changes in electrical conductivity or redox processes that can be observed and associated with glucose levels. The current study serves as a preliminary analysis, and further in vivo studies are necessary to evaluate the practical use of the synthesized nanoparticles for glucose sensing in physiologically relevant ranges. Biosynthesized nickel nanoparticles may be more biocompatible than those made chemically and they should attract interest because they may improve the sensitivity and specificity of glucose sensors. Present study shows that metal nanoparticles can be used as a highly sensitive electrochemical sensor for glucose sensing.

3.3.6 Anti-bacterial assay

In the current study, the disc diffusion assay was employed to investigate the antibacterial properties. The impact of LNiNPs on the growth of both Gram-negative bacteria (*Klebsiella pneumoniae*- ATCC 33591) and Gram-positive bacteria (*Staphylococcus aureus*- ATCC 700603) was assessed. Control plates loaded with solvent (25 µg) exhibited a zone of inhibition (ZOI) measuring 5.6 mm. However, when filter papers infused with LNiNPs concentrations of 5 µg, 10 µg, 15 µg, and 20 µg were used, the diameter of the inhibition zone showed a range of 7.3 mm, 8.66 mm, 10.6 mm, and 12.6 mm, respectively, for *K. pneumoniae* (as depicted in Table 2 & Fig. 10a, b). In the case of *S. aureus*, the ZOI for the control (25 µg) was 9.33 mm, while filter papers containing 5 µg, 10 µg, 15 µg, and 20 µg of LNiNPs exhibited inhibition zone diameters of 12.6 mm, 14.3 mm, 16.67 mm, and 19 mm, respectively. This trend indicates

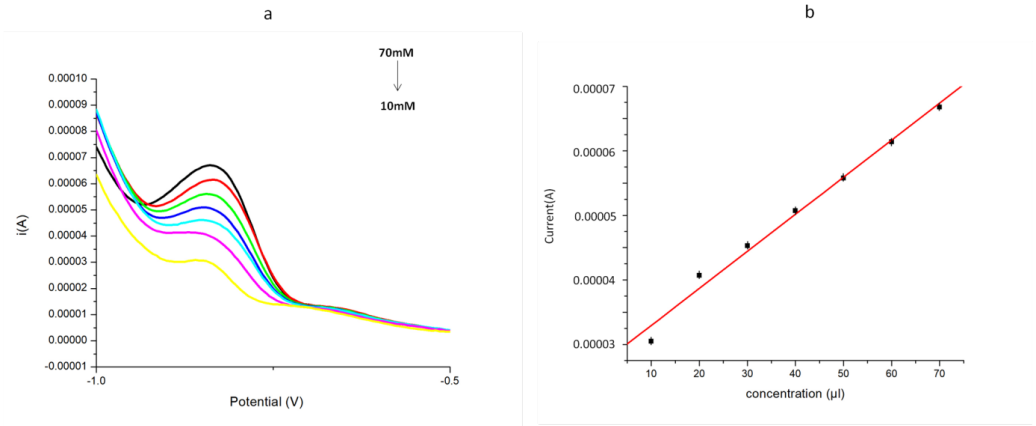

Figure 9. Electrochemical sensing of glucose (a) Sensing of glucose by DPV method. (b) Calibration curve of DPV method.

Table 2. LNiNPs mediated diameter of ZOI of *S. aureus* & *K. pneumoniae*.

Treatment	Concentration (µg)	*S.aureus* (mm ± SD)	*K.pneumonia* (mm ± SD)
Control	25 μg	9.33 ± 0.58	5.66 ± 0.57
Experiment	5 μg	12.67 ± 0.58	7.33 ± 0.57
	10 μg	14.33 ± 0.58	8.66 ± 0.57
	15 μg	16.67 ± 0.58	10.66 ± 0.57
	20 μg	19.00 ± 0.58	12.66 ± 0.57

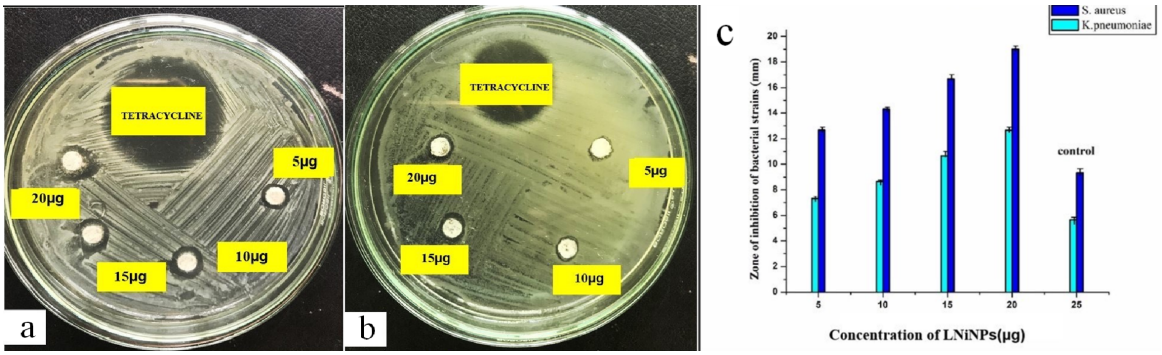

Figure 10. Antibacterial activity of LNiNPs (a) Zone of inhibition of *S. aureus* (b) *K. pneumoniae* by the action of LNiNPs and (c) Comparison graph showing effect of LNiNPs on both strains of bacteria.

an incremental increase in the diameter of the inhibition zone with an ascending concentration of LNiNPs, as shown in Fig. 10c. The antibacterial activity of LNiNPs is dose-dependent with increase in concentration of LNiNPs the antimicrobial activity increases at and the activity towards the *S. aureus* is greater when compared with *K. pneumoniae*. This finding is consistent with previous reports on the antibacterial properties of nanoparticles [70, 71] , including those synthesized from *Ocimum sanctum* [66].

3.3.7 Anti-oxidant activity (DPPH assay)

The DPPH assay, a widely accepted method for evaluating the capacity of nanoparticles to scavenge free radicals, has been extensively employed for assessing antioxidant activity. Various concentrations of LNiNPs (20 µg, 40 µg, 60 µg, 80 µg, 100 µg) were used for the analysis, each sample was combined with DPPH to create 2 mL solutions. Distilled water was used as the solvent for dissolving ascorbic acid, serving as the standard. Following a 30-minute incubation period in darkness, the solution was subjected to UV spectroscopy for analysis. The highest electron absorption of DPPH- free radicals was observed at 517 nm. Concentration-dependent scavenging activity of LNiNPs was documented in Table 3 and Fig. 11a. The concentration of the sample required to achieve 50% scavenging activity (EC_{50} value) was determined to be 48 µL (Fig. 11b). With an increase in the concentration of LNiNPs, the color of the DPPH transitioned from deep violet to pale yellow. UV spectroscopic analysis verified the heightened antioxidant potency of NiNPs at elevated concentrations, as indicated in

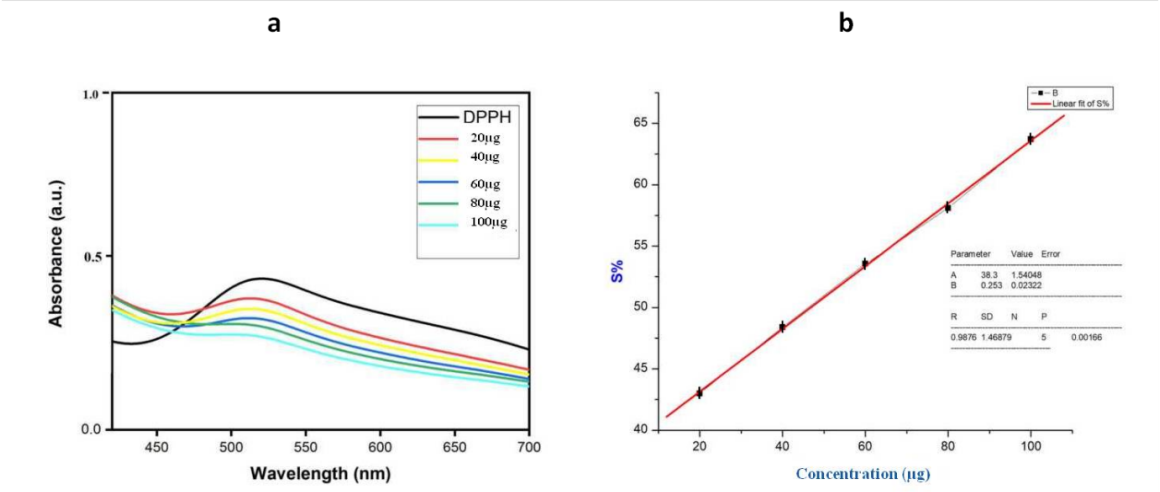

Figure 11. Antioxidant assay (a) DPPH activity of LNiNPs (b) calibration curve of LNiNPs.

Table 3. Concentration dependent scavenging activity of LNiNPs.

Concentration of LNiNPs (µg)	Absorbance of control	Absorbance Of LNiNPs mixed DPPH solution	S%
20	0.8	0.45 ± 0.01	43
40	0.8	0.41 ± 0.01	48.4
60	0.8	0.37 ± 0.01	53.56
80	0.8	0.33 ± 0.01	58.11
100	0.8	0.29 ± 0.01	63.7
		EC_{50}	48 µg

Table 3. UV spectroscopic research confirmed that NiNPs at higher doses have increased antioxidant potency. Similar findings have been reported in various studies within the field of bio-inspired synthesis of nickel nanoparticles [56, 71]. Reactive oxygen species (ROS) can form as a result of oxidation, a normal cellular process that can disrupt the cell's physiological balance. A lack of antioxidants can lead to harmful effects like lipid peroxidation, protein oxidation, enzyme inactivation, and DNA damage. Earlier investigations have regarded chemically synthesized nickel oxide nanoparticles as innovative antioxidants due to their capability to neutralize free radicals. Furthermore, it has been demonstrated that the efficiency of nickel oxide in scavenging free radicals is influenced by imperfections arising from its chemical production [67]. This study lends support to the capacity of bio-inspired nickel oxide nanoparticles to effectively neutralize free radicals. The antioxidant activity of LNiNPs was demonstrated through a concentration-dependent quenching of radicals using the DPPH free radical assay.

DPPH radical scavenging activity (S%) of the sample against concentration was plotted using the equation $S\% = [(A_{control} - A_{sample}) / A_{control}] \times 100$.

The concentration of sample required to produce 50% scavenging activity (EC_{50} value) obtained from the graph through linear regression equation.

3.3.8 Chromosomal aberration assay

The utilization of biosynthesized LNiNPs in chromosomal aberration studies strongly indicated the induction of phytotoxicity, resulting in the generation of chromosomal abnormalities (Fig. 12a, b). This observation was further supported by conspicuous evidence revealing a dose-dependent alteration in the proliferation of root cells upon exposure to various concentrations of LNiNPs ranging from 100 µg to 500 µg. The present investigation revealed distinct chromosomal anomalies including chromosome bridges, anaphase stickiness, vagrant chromosomes, broken chromosomes, and lag chromosomes as shown in Fig. 12(a1-d6) & (a-r). The genotoxic potential of LNiNPs was quantified as a percentage relative to both the control and experimental conditions. Analysis of the data indicated that the Mitotic Index (MI) in the control group remained within the normal range, whereas in the experimental group, the percentage of chromosomal abnormalities exhibited a gradual rise, accompanied by a declining % MI (Fig. 13a, b). According to the current study, onion bulbs exposed to varying concentrations of nanoparticles may have contained LNiNPs that, upon adhering to onion roots and infiltrating tissues, induced the generation of reactive oxygen species (ROS), consequently disrupting redox equilibrium and eliciting genotoxic and mito-depressive effects [72–74]. The phytotoxic capability of LNiNPs may potentially be harnessed

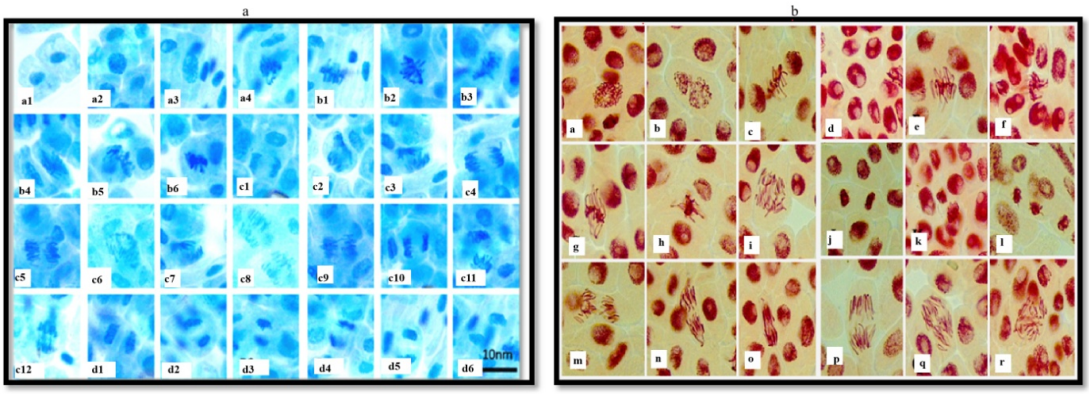

Figure 12. Chromosomal aberration assay (a) represents chromosomal aberrations in *Allium cepa* cells staines with methylene blue stain (a1) normal cell(a2) normal prophase (a3) disentegrated prophase (b1) normal metaphase (b2-b3) sticky metaphase (b4-b6) disturbed metaphase (c1) normal anaphase (c2) lag anaphase (c3) anaphase bridges (c4-c5) sticky anaphase (c6 – c9) broken chromosomes during anaphase (c10-c12) vagrant chromosomes in anaphase chromosome (d1) normal telophase (d2- d6) abnormal telophase Figure 12. (b) represents acetocarmine stain. (a) Normal prophase (b) Disintegrating prophase (c) Normal metaphase (e, f, g, h) Sticky & Laggered metaphase (d) Disintegrating nuclei (i) Sticky Anaphase (j) Normal telophase (k, l) Disoriented telophase (m, n) Chromosomal breakage during anaphase (o) Anaphase bridge (p,q) Laggered anaphase (r) Chromosome breakage .

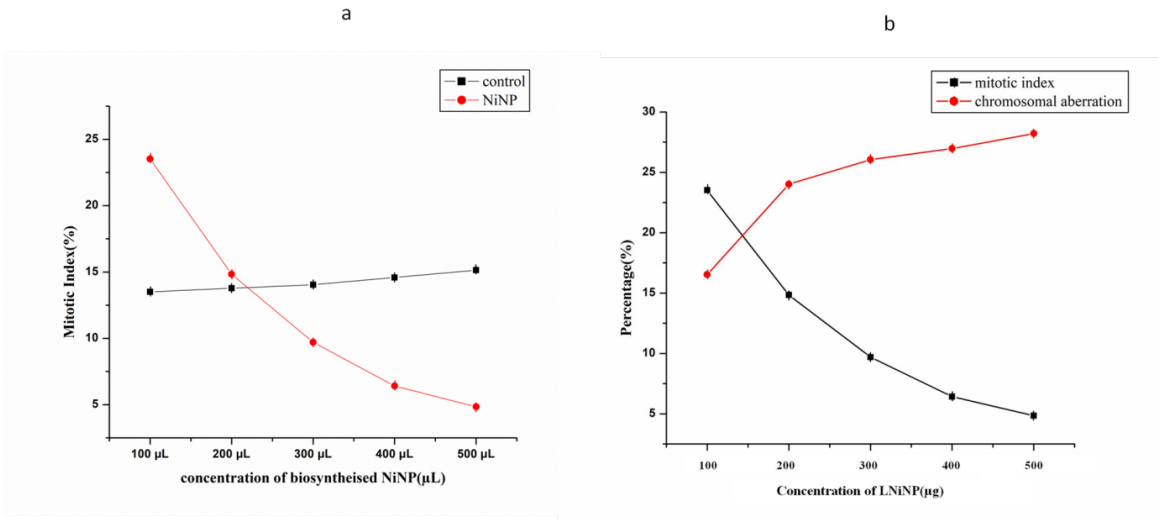

Figure 13. (a) Normal mitotic index of control and declined mitotic index of LNiNPs treated root cells. (b) Comparison of percentage of mitosis and chromosomal aberrations on LNiNPs treated root cells.

for the purpose of eradicating plant galls and tumors in the future.

3.3.9 Cytotoxicity

Numerous nanoparticles possess pharmacological and biochemical traits, such as antioxidant and anti-inflammatory traits, which might be involved in their anticarcinogenic and antimutagenic activities. Today, biologically produced nanoparticles are essential in the treatment of numerous illnesses, including cancer [75]. Present study showed the efficiency of biologically synthesized nickel nanoparticles as an anticancerous agent using Dalton's lymphoma ascites (DLA) cell lines in vitro. The LNiNPs shows dose-dependent cytotoxicity against DLA cells. The assay showed a gradual increase in cell death according to the concentration of LNiNPs (Fig. 14). The LNiNPs exhibit cytotoxicity against DLA cells in a manner that is dependent on the dose administered. As stated above, antioxidants are essential for the prevention of diseases brought on by the impacts of free radicals, as well as for the treatment and prevention of cancer. Antioxidants are a diverse group of molecular substances that interact with free radicals and neutralize them. Antioxidants can prevent and treat cancer by destroying free radicals. Thus, the current investigation confirms that biosynthesized LNiNPs are entirely anticancerous, consistent with previous research demonstrating the anti-tumor properties of NiNPs. Although earlier studies have shown that some metal nanoparticles from insect defensive secretions exhibit anticancer activity, the results align with our findings [76]. Dalton's Lymphoma Ascitic (DLA) cell lines are significantly cytotoxic to nickel nanoparticles (NiNPs), yet the exact processes are still unknown. Based on available data, it appears that NiNPs mostly cause oxidative stress, which results in the production of reactive oxygen species (ROS) that harm cellular constituents such proteins, lipids, and DNA and ultimately cause cell death. NiNPs may also damage cell membranes, resulting in leakage and necrosis, as well as incite inflammatory reactions that heighten cytotoxicity. The consequences that are detected are also influenced by DNA damage and the activation of apoptotic pathways, which includes mitochondrial malfunction. Notwithstanding these revelations, thorough mechanistic investigations are still required to completely comprehend the ways in which NiNPs engage with DLA cells and to clarify any possible safety concerns or therapeutic applications [77, 78].

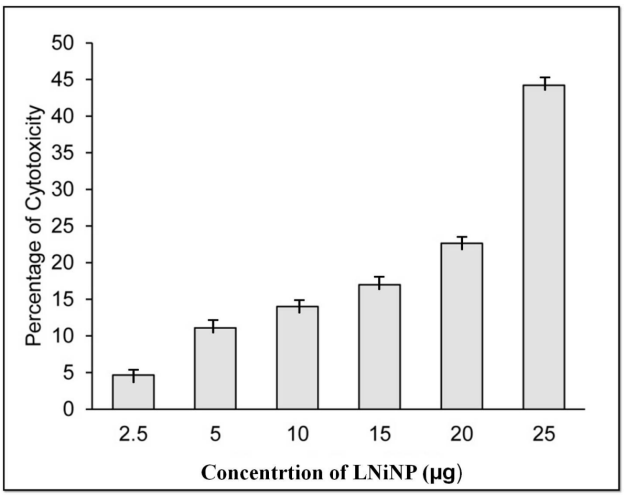

Figure 14. Anticancer property of LNiNPs on DLA cells.

4. Conclusion

In conclusion, this study endeavored to establish a direct method for the eco-friendly, cost-effective, and non-toxic synthesis of nickel nanoparticles, employing the insect *Luprops tristis* as a unique approach. The successful biosynthesis of nickel nanoparticles was verified through a comprehensive range of analytical techniques, including UV-Vis spectrometry, FTIR analysis, SEM, TEM, DLS and Zeta potential analysis. The nanoparticles exhibited an irregular spherical shape with a rough surface, possessing an average size of 18 nm and hydrodynamic size of approximately 48 nm. The findings of the study further

demonstrated the enzyme free glucose sensing of LNiNPs coated electrode used as a biosensor and dose-dependent antimicrobial impact of LNiNPs against the bacteria, *S. aureus* and *K. pneumoniae*, highlighting its potential as an effective bacterial inhibitor. Remarkably, the nanoparticles also induced chromosomal aberrations in the root tips of *Allium cepa*, with an increased concentration of nanoparticles leading to a reduced mitotic index and heightened chromosomal aberrations. Additionally, the study unveiled the antioxidative potential of LNiNPs and established their dose-dependent cytotoxicity against DLA cells. This comprehensive evaluation emphasized the versatility of biosynthesized nickel nanoparticles in various applications, including antimicrobial and antioxidant properties, as well as potential applications in biosensing and cancer therapy.

Acknowledgement

The first author, O. Sabira, gratefully acknowledges the financial support provided by the Council of Scientific and Industrial Research, New Delhi, India, which was instrumental in the successful completion of this research article. We extend our sincere thanks to STIC CUSAT Cochin, India for TEM analysis, CSIF - University of Calicut, India for SEM analysiz, and Amala Cancer Research Centre, Thrissur, India for anticancer study.

Authors contributions
Authors have contributed equally in preparing and writing the manuscript.

Availability of data and materials
The data generated and analyzed during the current study are available from the corresponding author upon reasonable request.

Conflict of interests
The authors declare that they have no known competing financial interests or personal relationships that could have appeared to influence the work reported in this paper.

References

[1] A. Angel Ezhilarasi, J. Judith Vijaya, K. Kaviyarasu, L. John Kennedy, R. J. Ramalingam, and H. A. Al-Lohedan. "Green synthesis of NiO nanoparticles using aegle marmelos Leaf Extract for the Evaluation of In-Vitro cytotoxicity, antibacterial and photocatalytic properties.". *Journal of Photochemistry and Photobiology B: Biology*, 180(1):39–50, 2018.
DOI: https://doi.org/10.1016/j.jphotobiol.2018.01.023.

[2] I. Bibi, S. Kamal, A. Ahmed, M. Iqbal, S. Nouren, K. Jilani, N. Nazar, M. Amir, A. Abbas, S. Ata, and F. Majid. "Nickel nanoparticle synthesis using Camellia Sinensis as reducing and capping agent: Growth mechanism and photo-catalytic activity evaluation.". *International Journal of Biological Macromolecules*, 103:783–790, 2017.
DOI: https://doi.org/10.1016/j.ijbiomac.2017.05.023.

[3] R. Abu-Much and A. Gedanken. "Sonochemical synthesis under a magnetic field: Fabrication of nickel and cobalt particles and variation of their physical properties.". *Chemistry - A European Journal*, 14(32):10115–10122, 2008.
DOI: https://doi.org/10.1002/chem.200801469.

[4] M. Alimoradi, M. Yousefi, B. Sadeghi, M. M. Amini, and A. Abbasi. "Structural and magnetic behavior of BaAlxCryFe11O19 (x + y = 1) Hexagonal Ferrites.". *Journal of Superconductivity and Novel Magnetism*, 32(8):2533–2538, 2019.
DOI: https://doi.org/10.1007/s10948-018-4980-5.

[5] A. P. Ajaykumar, A. Mathew, A. P. Chandni, S. R. Varma, K. N. Jayaraj, O. Sabira, V. A. Rasheed, V. S. Binitha, T. R. Swaminathan, V. S. Basheer, S. Giri, and S. Chatterjee. "Green synthesis of silver nanoparticles using the Leaf Extract of the Medicinal Plant, Uvaria narum and its antibacterial, antiangiogenic, anticancer and catalytic properties.". *Antibiotics*, 12(3), 2023.
DOI: https://doi.org/10.3390/antibiotics12030564.

[6] M. Iqbal. "Vicia Faba bioassay for environmental toxicity monitoring: A review.". *Chemosphere*, 144(1):785–802, 2016.
DOI: https://doi.org/10.1016/j.chemosphere.2015.09.048.

[7] P. Kuppusamy, M. M. Yusoff, G. P. Maniam, and N. Govindan. "Biosynthesis of metallic nanoparticles using plant derivatives and their new Avenues in pharmacological applications - an updated report.". *Saudi Pharmaceutical Journal*, 24(4):473–484, 2016.
DOI: https://doi.org/10.1016/j.jsps.2014.11.013.

[8] H. Khodadad, F. Hatamjafari, K. Pourshamsian, and B. Sadeghi. "Microwave-assisted synthesis of novel pyrazole derivatives and their biological evaluation as anti-bacterial agents.". *Combinatorial Chemistry & High Throughput Screening*, 24(5):695–700, 2021.
DOI: https://doi.org/10.2174/1386207323666201019152206.

[9] N. Matinise, X. G. Fuku, K. Kaviyarasu, N. Mayedwa, and M. Maaza. "ZnO nanoparticles via Moringa Oleifera green synthesis: Physical properties & mechanism of formation.". *Applied Surface Science*, 406:339–347, 2017.
DOI: https://doi.org/10.1016/j.apsusc.2017.01.219.

[10] F. Tavakoli, M. Salavati-Niasari, D. Ghanbari, K. Saberyan, and S. M. Hosseinpour-Mashkani. "Application of glucose as a green capping agent and reductant to fabricate CuI micro/nanostructures.". *Materials Research Bulletin*, 49(1):14–20, 2014.
DOI: https://doi.org/10.1016/j.materresbull.2013.08.037.

[11] B. Koul, A. K. Poonia, D. Yadav, and J.-O. Jin. "Microbe-mediated biosynthesis of nanoparticles: Applications and future prospects.". *Biomolecules*, 11(6), 2021.
DOI: https://doi.org/10.3390/biom11060886.

[12] I. Din and A. Rani. "Recent advances in the synthesis and stabilization of nickel and nickel oxide nanoparticles: A green adeptness". *International Journal of Analytical Chemistry*, 2016(1):1–14, 2016.
DOI: https://doi.org/10.1155/2016/3512145.

[13] M. Anjaly, A. R. Ramesh, A. R. Vazhanthodi, B. V. Sivadasan, S. Ovungal, S. M. Subrahmanian, P. Chittadimangalath, and A. A. Parambil. "Microwave-assisted greener synthesis of silver nanoparticles using Entada Rheedii Leaf Extract and investigation of its anticancer and antimicrobial properties.". *Int. J. Nano Dimens.Int. J. Nano Dimens.*, 13:329–334, 2022.
DOI: https://doi.org/10.22034/ijnd.2022.1952713.2126.

[14] M. E. Elnosary, H. A. Aboelmagd, M. A. Habaka, S. R. Salem, and M. E. El-Naggar. "Synthesis of bee venom loaded chitosan nanoparticles for anti-MERS-COV and multi-drug resistance bacteria.". *International Journal of Biological Macromolecules*, 224: 871–880, 2023.

[15] N. Mohammad pourdounighi, A. Behfar, A. Ezabadi, H. Zolfagharian, and M. Heydari. "Preparation of chitosan nanoparticles containing Naja naja oxiana snake venom.". *Nanomedicine: Nanotechnology, Biology and Medicine*, 6(1):137–143, 2010.

[16] S. A. Nisa, K. Govindaraju, R. Vasantharaja, M. Kannan, and K. Raja. "Jellyfish Acromitus flagellatus (Maas) nematocyst venom-mediated biogenic synthesis of gold nanoparticles and its anti-proliferative effects.". *Aquaculture International*, 31(4):2235–2244, 2023.

[17] E. Y. Ahn, S. J. Hwang, M. J. Choi, S. Cho, H. J. Lee, and Y. Park. "Upcycling of jellyfish (Nemopilema nomurai) sea wastes as highly valuable reducing agents for green synthesis of gold nanoparticles and their antitumor and anti-inflammatory activity.". *Artificial cells, nanomedicine, and biotechnology*, 46(sup2):1127–1136, 2018.

[18] R. K. Singha, A. Yadav, A. Agrawal, A. Shukla, S. Adak, T. Sasaki, and R. Bal. "Synthesis of highly coke resistant Ni nanoparticles supported MgO/ZnO catalyst for reforming of methane with carbon dioxide.". *Applied Catalysis B: Environmental*, 191(1):165–178, 2016.
DOI: https://doi.org/10.1016/j.apcatb.2016.03.029.

[19] N.-D. Jaji, H. L. Lee, M. H. Hussin, H. M. Akil, M. R. Zakaria, and M. B. H. Othman. "Advanced nickel nanoparticles technology: From synthesis to applications.". *Nanotechnology Reviews*, 9(1): 1456–1480, 2020.
DOI: https://doi.org/10.1515/ntrev-2020-0109.

[20] H. Wang, X. Jiao, and D. Chen. "Monodispersed nickel nanoparticles with tunable phase and size: Synthesis, characterization, and magnetic properties.". *The Journal of Physical Chemistry C*, 112 (48):18793–18797, 2008.
DOI: https://doi.org/10.1021/jp805591y.

[21] Y.-M. Yan, L.-J. Li, X.-C. Qin, Q. Lu, Z.-C. Tu, and Y.-X. Cheng. "Compounds from the insect Blaps japanensis with COX-1 and COX-2 inhibitory activities.". *Bioorganic & Medicinal Chemistry Letters*, 25(12):2469–2472, 2015.
DOI: https://doi.org/10.1016/j.bmcl.2015.04.085.

[22] S. L. Gafner and Yu. Ya. Gafner. "Analysis of gas-phase condensation of nickel nanoparticles.". *Journal of Experimental and Theoretical Physics*, 107(4):712–722, 2008.
DOI: https://doi.org/10.1134/S1063776108100191.

[23] H.N. Bhatti, Q. Zaman, A. Kausar, S. Noreen, and M. Iqbal. "Efficient remediation of Zr(IV) using citrus peel waste biomass: Kinetic, equilibrium and thermodynamic studies.". *Ecological Engineering*, 95(1):216–228, 2016.
DOI: https://doi.org/10.1016/j.ecoleng.2016.06.087.

[24] D. Fan, J. Feng, S. Zhang, X. Lv, T. Gao, J. Xie, and J. Liu. "Synthesis, structure, and magnetic properties of Ni and Co nanoparticles encapsulated by few-layer h-BN.". *Journal of Alloys and Compounds*, 689:153–160, 2016.
DOI: https://doi.org/10.1016/j.jallcom.2016.07.279.

[25] A. Babarinde and G. O. Onyiaocha. "Equilibrium sorption of divalent metal ions onto groundnut (Arachis hypogaea) shell: Kinetics, isotherm and thermodynamics.". *Chem. Int*, 2(3):37–46, 2016.

[26] A. Dzimitrowicz, P. Jamróz, G. C. diCenzo, I. Sergiel, T. Kozlecki, and P. Pohl. "Preparation and characterization of gold nanoparticles prepared with aqueous extracts of Lamiaceae plants and the effect of follow-up treatment with atmospheric pressure glow microdischarge.". *Arabian Journal of Chemistry*, 12(8):4118–4130, 2019.
DOI: https://doi.org/10.1016/j.arabjc.2016.04.004.

[27] K.-B. Lee, S. Park, and C. A. Mirkin. "Multicomponent magnetic nanorods for biomolecular separations.". *Angewandte Chemie International Edition*, 43(23):3048–3050, 2004.
DOI: https://doi.org/10.1002/anie.200454088.

[28] J. Iqbal, B. A. Abbasi, T. Mahmood, S. Hameed, A. Munir, and S. Kanwal. "Green synthesis and characterizations of Nickel oxide nanoparticles using leaf extract of *Rhamnus virgata* and their potential biological applications.". *Applied Organometallic Chemistry*, 33 (8), 2019.
DOI: https://doi.org/10.1002/aoc.4950.

[29] M. Ntwasa, A. Goto, and S. Kurata. "Coleopteran antimicrobial peptides: Prospects for clinical applications.". *International Journal of Microbiology*, 2012(101989):1–9, 2012.
DOI: https://doi.org/10.1155/2012/101989.

[30] C.-C. Li, F.-S. Yu, M.-J. Fan, Y.-Y. Chen, J.-C. Lien, Y.-C. Chou, H.-F. Lu, N.-Y. Tang, S.-F. Peng, W.-W. Huang, and J.-G. Chung. "Anticancer effects of cantharidin in A431 human skin cancer (Epidermoid carcinoma) cells in vitro and in vivo.". *Environmental Toxicology*, 32(3):723–738, 2017.
DOI: https://doi.org/10.1002/tox.22273.

[31] S. Yan, D. Sun, Y. Tan, X. Xing, H. Yu, and Z. Wu. "Synthesis and formation mechanism of Ag–Ni alloy nanoparticles at room temperature.". *Journal of Physics and Chemistry of Solids*, 98(1): 107–114, 2016.
DOI: https://doi.org/10.1016/j.jpcs.2016.06.013.

[32] A. Ali and O. Rakha. "Paederus Alfieri extract induces apoptosis in Human Myeloid Leukemia K562 Cells.". *Asian J Pharm Clin Res*, 10(1):1–4, 2017.
DOI: https://doi.org/10.22159/ajpcr.2017.v10i1.13513.

[33] T. Magrone, M. A. Russo, and E. Jirillo. "Antimicrobial peptides: Phylogenic sources and biological activities. First of two parts.". *Current Pharmaceutical Design*, 24(10):1043–1053, 2018.
DOI: https://doi.org/10.2174/1381612824666180403123736.

[34] Z. Adamski, S. A. Bufo, S. Chowański, P. Falabella, J. Lubawy, P. Marciniak, J. Pacholska-Bogalska, R. Salvia, L. Scrano, M. Słocińska, M. Spochacz, M. Szymczak, A. Urbański, K. Walkowiak-Nowicka, and G. Rosiński. "Beetles as model organisms in physiological, biomedical and environmental studies - A review.". *Frontiers in Physiology*, 10(319):1–22, 2019.

[35] M. Nenadić, M. Soković, J. Glamočlija, A. Ćirić, V. Perić-Mataruga, L. Ilijin, V. Tešević, L. Vujisić, M. Todosijević, N. Vesović, and S. Ćurčić. "Antimicrobial activity of the pygidial gland secretion of three ground beetle species (Insecta: Coleoptera: Carabidae).". *The Science of Nature*, 103(3):34, 2016.
DOI: https://doi.org/10.1007/s00114-016-1358-z.

[36] L. Seabrooks and L. Hu. "Insects: An underrepresented resource for the discovery of biologically active natural products.". *Acta Pharmaceutica Sinica B*, 7(4):409–426, 2017.
DOI: https://doi.org/10.1016/j.apsb.2017.05.001.

[37] K. M. Barnes, D. E. Gennard, and R. A. Dixon. "An assessment of the antibacterial activity in larval excretion/secretion of four species of insects recorded in association with corpses, using Lucilia sericata Meigen as the marker species.". *Bulletin of Entomological Research*, 100(6):635–640, 2010.
DOI: https://doi.org/10.1017/S000748530999071X.

[38] N. Vesović, M. Nenadić, S. Vranić, L. Vujisić, K. M. Milinčić, M. Todosijević, I. Dimkić, T. Janakiev, N. B. Ćurčić, N. Stevanović, L. Mihajlović, D. Z. Vukoičić, and S. Ćurčić. "The chemical composition of the secretions, their antibacterial activity, and the pygidial gland morphology of selected european Carabini ground Beetles (Coleoptera: Carabidae).". *Frontiers in Ecology and Evolution*, 11 (1120006):1–13, 2023.

[39] C. L. Hall, N. K. Wadsworth, D. R. Howard, E. M. Jennings, L. D. Farrell, T. S. Magnuson, and R. J. Smith. "Inhibition of microorganisms on a carrion Breeding resource: The antimicrobial peptide activity of Burying Beetle (Coleoptera: Silphidae) Oral and Anal Secretions.". *Environmental Entomology*, 40(3):669–678, 2011.
DOI: https://doi.org/10.1603/EN10137.

[40] A. P. Ajaykumar, O. Sabira, M. Sebastian, S. R. Varma, K. B. Roy, V. S. Binitha, V. A. Rasheed, K. N. Jayaraj, and A. R. Vignesh. "A novel approach for the biosynthesis of silver nanoparticles using the defensive gland extracts of the beetle, Luprops tristis Fabricius.". *Scientific Reports*, 13(1):10186, 2023.
DOI: https://doi.org/10.1038/s41598-023-37175-0.

[41] P. Ajaykumar, A. Nikhila, K. Sabira, O. Narayanan Jayaraj, K. Rama Varma, S. A. Rasheed, V. S. Binitha, V. Sreeja, K. M. R. Ramakrishnan, and A. Babu. "A bio-inspired approach for the synthesis of few-layer graphene using beetle defensive gland extract.". *RSC Advances*, 14(9):5729–5739, 2024.
DOI: https://doi.org/10.1039/D3RA08733F.

[42] O. Sabira, A. R. Vignesh, A. P. Ajaykumar, S. R. Varma, K. N. Jayaraj, M. Sebastin, K. Nikhila, A. Babu, V. A. Rasheed, V. S. Binitha, Z. Vasu, koldath, and M. S. Sujith. "The chemical composition and antimitotic, antioxidant, antibacterial and cytotoxic properties of the defensive gland extract of the Beetle, Luprops tristis Fabricius.". *Molecules*, 27(21), 2022.
DOI: https://doi.org/10.3390/molecules27217476.

[43] A. P. Ajaykumar, O. Sabira, V. S. Binitha, S. R. Varma, A. Mathew, K. N. Jayaraj, P. A. Janish, K. V. Zeena, P. Sheena, V. Venugopal, P. Palakkapparambil, and Aswathi. "Bio-Fabricated silver nanoparticles from the leaf extract of the Poisonous Plant, Holigarna arnottiana: Assessment of antimicrobial, antimitotic, anticancer, and radical-scavenging properties.". *Pharmaceutics*, 15(10), 2023.
DOI: https://doi.org/10.3390/pharmaceutics15102468.

[44] B. Ahmed, M. Shahid, M. S. Khan, and J. Musarrat. "Chromosomal aberrations, cell Suppression and oxidative stress generation induced by metal oxide nanoparticles in onion (Allium Cepa) Bulb". *Metallomics*, 10(9):1315–1327, 2018.
DOI: https://doi.org/10.1039/c8mt00093j.

[45] O. Sabira, N. Drisya, A. P. Ajaykumar, A. Mathew, K. Narayanan Jayaraj, V. S. Binitha, and K. P. Viswanathan. "From Ficus recemosa Leaf Galls to Therapeutic silver nanoparticles: Antibacterial and anticancer applications.". *Pharmaceutics*, 16(8):1025, 2024.

[46] M. K. Choudhari, R. Haghniaz, J. M. Rajwade, and K. M. Paknikar. "Anticancer activity of Indian stingless bee propolis: an in vitro study.". *Evidence-Based Complementary and Alternative Medicine*, 2013(1):928280, 2013.

[47] S. Muthukrishnan, B. Vellingiri, and G. Murugesan. "Anticancer effects of silver nanoparticles encapsulated by Gloriosa superba (L.) leaf extracts in DLA tumor cells.". *Future Journal of Pharmaceutical Sciences*, 4(2):206–214, 2018.

[48] S. M. Helen and M. H. E. Rani. "Characterization and antimicrobial study of nickel nanoparticles synthesized from dioscorea (Elephant Yam) by green route.". *International Journal of Science and Research*, 4(11):216–219, 2015.

[49] S. Chandra, A. Kumar, and P. K. Tomar. "Synthesis of Ni nanoparticles and their characterizations.". *Journal of Saudi Chemical Society*, 18(5):437–442, 2014.
DOI: https://doi.org/10.1016/j.jscs.2011.09.008.

[50] N. Jamila, N. Khan, A. Bibi, A. Haider, S. Noor Khan, A. Atlas, U. Nishan, A. Minhaz, F. Javed, and A. Bibi. "Piper longum catkin extract mediated synthesis of Ag, Cu, and Ni nanoparticles and their applications as biological and environmental remediation agents.". *Arabian Journal of Chemistry*, 13(8):6425–6436, 2020.
DOI: https://doi.org/10.1016/j.arabjc.2020.06.001.

[51] J. K. Patra and K.-H. Baek. "Green nanobiotechnology: Factors affecting synthesis and characterization techniques.". *Journal of Nanomaterials*, 2014(1):1–12, 2014.
DOI: https://doi.org/10.1155/2014/417305.

[52] S. Shankar and J.-W. Rhim. "Amino acid mediated synthesis of silver nanoparticles and preparation of antimicrobial agar/silver nanoparticles composite films.". *Carbohydrate Polymers*, 130(1):353–363, 2015.
DOI: https://doi.org/10.1016/j.carbpol.2015.05.018.

[53] R.S. Tomar, P. Chauhan, and V. Shrivastava. " Critical review on nanoparticle synthesis: Physicochemical V/s biological approach.". *World Journal of Pharmaceutical Research*, 4(1):595–620, 2015.

[54] C. Yuan, B. Jiang, X. Xu, Y. Wan, L. Wang, and J. Chen. "Anti-human ovarian cancer and cytotoxicity effects of nickel nanoparticles green-synthesized by *Alhagi maurorum* leaf aqueous extract.". *Journal of Experimental Nanoscience*, 17(1):113–125, 2022.
DOI: https://doi.org/10.1080/17458080.2021.2011860.

[55] Y. Duan and J. Li. "Structure study of nickel nanoparticles.". *Materials Chemistry and Physics*, 87(2-3):452–454, 2004.
DOI: https://doi.org/10.1016/j.matchemphys.2004.06.034.

[56] P. Adwin Jose, J. Dhaveethu Raja, and M. Sankarganesh J. Rajesh. "Evaluation of antioxidant, DNA targeting, antimicrobial and cytotoxic studies of imine capped copper and nickel nanoparticles.". *Journal of Photochemistry and Photobiology B: Biology*, 178(1): 143–151, 2018.
DOI: https://doi.org/10.1016/j.jphotobiol.2017.11.005.

[57] G. Rajakumar, A. A. Rahuman, K. Velayutham, J. Ramyadevi, K. Jeyasubramanian, A. Marikani, G. Elango, C. Kamaraj, T. Santhoshkumar, S. Marimuthu, A. A. Zahir, A. Bagavan, C. Jayaseelan, A. V. Kirthi, M. Iyappan, and C. Siva. "Novel and simple approach using synthesized nickel nanoparticles to control blood-sucking parasites.". *Veterinary Parasitology*, 191(3-4):332–339, 2013.
DOI: https://doi.org/10.1016/j.vetpar.2012.08.028.

[58] Y. Hou, H. Kondoh, T. Ohta, and S. Gao. "Size-controlled synthesis of nickel nanoparticles.". *Applied Surface Science*, 241(1-2):218–222, 2005.
DOI: https://doi.org/10.1016/j.apsusc.2004.09.045.

[59] J. D. Clogston and A. K. Patri. "Zeta potential measurement. In S. E. McNeil (Ed.)". *Characterization of Nanoparticles Intended for Drug Delivery*, 697:63–70, 2011.
DOI: https://doi.org/10.1007/978-1-60327-198-1-6.

[60] G. Elango, S. M. Roopan, K. I. Dhamodaran, K. Elumalai, N. A. Al-Dhabi, and M. V. Arasu. "Spectroscopic investigation of biosynthesized nickel nanoparticles and its Larvicidal, Pesticidal activities.". *Journal of Photochemistry and Photobiology B: Biology*, 162(1):162–167, 2016.
DOI: https://doi.org/10.1016/j.jphotobiol.2016.06.045.

[61] S. Honary and F. Zahir. "Effect of zeta potential on the properties of nano-drug delivery systems-A review (Part 1).". *Tropical Journal of Pharmaceutical Research*, 12(2):255–264, 2013.
DOI: https://doi.org/10.4314/tjpr.v12i2.19.

[62] D. L. Liao, G. S. Wu, and B. Q. Liao. "Zeta potential of shape-controlled TiO_2 nanoparticles with surfactants.". *Colloids and Surfaces A: Physicochemical and Engineering Aspects*, 348(1):270–275, 2009.
DOI: https://doi.org/10.1016/j.colsurfa.2009.07.036.

[63] V. Sharma, C. Chotia, Tarachand, V. Ganesan, and G. S. Okram. "Influence of particle size and dielectric environment on the dispersion behaviour and surface plasmon in nickel nanoparticles.". *Physical Chemistry Chemical Physics*, 19(21):14096–14106, 2017.
DOI: https://doi.org/10.1039/C7CP01769C.

[64] A. Doostmohammadi, A. Monshi, R. Salehi, M. H. Fathi, Z. Golniya, Daniels, and U. Alma. "Bioactive glass nanoparticles with negative zeta potential.". *Ceramics International*, 37(7):2311–2316, 2011.
DOI: https://doi.org/10.1016/j.ceramint.2011.03.026.

[65] F. Shahbazi, R. Ahmadi, M. Noghani, and G. Karimi. "Antibacterial activity of the Iron-Zinc Oxide nanoparticles synthesized via electric discharge method.". *International Journal of Nano Dimension*, 14 (1):60–72, 2023.
DOI: https://doi.org/10.22034/ijnd.2022.1962974.2158.

[66] C. Jeyaraj Pandian, R. Palanivel, and S. Dhanasekaran. "Screening antimicrobial activity of nickel nanoparticles synthesized using *Ocimum sanctum* leaf extract.". *Journal of Nanoparticles*, 2016:1–13, 2016.
DOI: https://doi.org/10.1155/2016/4694367.

[67] Md. Moulana Kareem, H. Babu, and G. Vijaya Lakshmi. "Anticancer, antibacterial, antioxidant, and photo-catalytic activities of eco-friendly synthesized Ni nanoparticles". *Inorganic Chemistry Communications*, 148:110274, 2023.
DOI: https://doi.org/10.1016/j.inoche.2022.110274.

[68] S. Coster, M. C. Gulliford, P. T. Seed, J. K. Powrie, and R. Swaminathan. "Monitoring blood glucose control in diabetes mellitus: A systematic review.". *Health Technology Assessment (Winchester, England)*, 4(12):1–93, 2000.

[69] M.-S. Steiner, A. Duerkop, and O. S. Wolfbeis. "Optical methods for sensing glucose.". *Chemical Society Reviews*, 40(9):4805–4839, 2011.
DOI: https://doi.org/10.1039/C1CS15063D.

[70] R. A. Gomaji Chaudhary, J. V. Tanna, N. R. Gandhare, A. D. Rai, and H. Juneja. "Synthesis of nickel nanoparticles: Microscopic investigation, an efficient catalyst and effective antibacterial activity.". *Advanced Materials Letters*, 6(11):990–998, 2015. DOI: https://doi.org/10.5185/amlett.2015.5901.

[71] A. H. Hashem, M. A. Al Abboud, M. M. Alawlaqi, T. M. Abdelghany, and M. Hasanin. "Synthesis of nanocapsules based on biosynthesized nickel nanoparticles and potato starch: Antimicrobial, antioxidant, and anticancer activity.". *Starch - Stärke*, 74(1-2):2100165, 2022. DOI: https://doi.org/10.1002/star.202100165.

[72] A. De, M. Chakrabarti, I. Ghosh, and A. Mukherjee. "Evaluation of genotoxicity and oxidative stress of aluminium oxide nanoparticles and its bulk form in Allium cepa.". *The Nucleus*, 59(3):219–225, 2016. DOI: https://doi.org/10.1007/s13237-016-0179-y.

[73] R. Liman, M. M. Ali, E. S. Istifli, I. H. Ciğerci, and E. Bonciu. "Genotoxic and cytotoxic effects of pethoxamid herbicide on Allium cepa cells and its molecular docking studies to unravel genotoxicity mechanism.". *Environmental Science and Pollution Research*, 29 (42):63127–63140, 2022. DOI: https://doi.org/10.1007/s11356-022-20166-5.

[74] Q. Wang, S. D. Ebbs, Y. Chen, and X. Ma. "Trans-generational impact of cerium oxide nanoparticles on tomato plants.". *Metallomics*, 5(6):753, 2013. DOI: https://doi.org/10.1039/c3mt00033h.

[75] P. Rameshthangam and J. P. Chitra. "Synergistic anticancer effect of green synthesized nickel nanoparticles and quercetin extracted from Ocimum sanctum leaf extract.". *Journal of Materials Science & Technology*, 34(3):508–522, 2018. DOI: https://doi.org/10.1016/j.jmst.2017.01.004.

[76] O. Sabira and A. Anthyalam Parambil. "Bio-synthesis of Copper Oxide nanoparticles using beetle defensive gland extract: Exploring diverse applications.". *International Journal of Nano Dimension (Int. J. Nano Dimens.)*, 659(2024):e844f1d071, 2024. DOI: https://doi.org/10.57647/j.ijnd.2024.1503.21.

[77] S. S. Sana, R. P. Singh, M. Sharma, A. K. Srivastava, G. Manchanda, A. R. Rai, and Z. J. Zhang. "Biogenesis and application of nickel nanoparticles: a review.". *Current Pharmaceutical Biotechnology*, 22(6):808–822, 2021.

[78] M. G. Berhe and Y. T. Gebreslassie. "Biomedical applications of biosynthesized nickel oxide nanoparticles.". *International Journal of Nanomedicine*, pages 4229–4251, 2023.